Received: 4 February 2021 | Revised: 9 June 2021 | Accepted: 12 June 2021

DOI: 10.1111/ijag.16262

INTERNATIONAL JOURNAL OF Applied Glass SCIENCE

SPECIAL ISSUE ARTICLE

# New glass-based binders from engineered mixtures of inorganic waste

**Miroslava Hujova[1] | Patricia Rabelo Monich[2] | Hana Kankova[1] | Hugo Lucas[3] | Buhle Xakalashe[3,4] | Bernd Friedrich[3] | Jozef Kraxner[1] | Dusan Galusek[1,5] | Enrico Bernardo[2]**

[1]FunGlass—Centre for Functional and Surface Functionalized Glass, Alexander Dubček University of Trenčín, Trenčín, Slovakia

[2]Department of Industrial Engineering, University of Padova, Padova, Italy

[3]IME Process Metallurgy and Metal Recycling, RWTH Aachen University, Aachen, Germany

[4]Pyrometallurgy Division, MINTEK, Randburg, South Africa

[5]Joint Glass Centre of the IIC SAS, TnUAD, and FChFT STU, Trenčín, Slovakia

**Correspondence**
Miroslava Hujova, FunGlass—Centre for Functional and Surface Functionalized Glass, Alexander Dubček University of Trenčín, Trenčín, Slovakia.
Email: miroslava.hujova@tnuni.sk

**Funding information**
Vedecká Grantová Agentúra MŠVVaŠ SR a SAV, Grant/Award Number: Nr 2/0091/20; Horizon 2020 Framework Programme, Grant/Award Number: 721185 and 739566

**Abstract**

Aluminum is one of the most important strategic resources, but the Bayer process, typically applied for the purification of ores, leads to vast amounts of alkaline slurry waste, known as red mud. Though interesting for potential reprocessing, red mud is still predominantly stored in big slurry pools, due to high levels of toxic metals. Toxic ions can be easily immobilized by vitrification, but the high costs of this solution need to be balanced by the reuse of the obtained glass. The present paper is dedicated to the transformation of waste-derived glass into new binders for the construction industry, according to both "conventional melting" and "smelting" approaches. In the first case, red mud was included in a mixture of waste, designed to yield a reactive glass (CMG), that is, forming stable gels after activation in an alkaline aqueous solution. In the second approach, red mud was subjected to a thermal treatment in a reductive atmosphere, implying the separation of molten iron alloy. The remaining glassy slag, according to its chemical composition (CaO and $Al_2O_3$-rich) underwent gelation by simple interaction with pure water, without any alkaline activator, thus configuring a new "glass cement."

**KEYWORDS**

alkali activation, alumino-silicate glasses, gelation, leaching, waste stabilization

## 1 | INTRODUCTION

Aluminum hydroxide, used as raw material in the processing of alumina ceramics and metallic aluminum, is not naturally available in pure form. It is typically separated from other minerals through the Bayer process, which produces a large amount of inorganic waste. Globally, every tonne of alumina produced implies between 1 and 1.5 tonnes of red mud.[1] The waste deriving from the Bayer process, usually termed as "red mud," is a caustic slurry, containing $Al_2O_3$ (5-30wt.%), $SiO_2$ (3-50wt.%), and $Fe_2O_3$ (5-60wt.%) as major components, but also featuring toxic pollutants, in the form of heavy metal (Cr, Ni, Cu, Pb, etc.) oxides.[2]

The handling of highly toxic constituents hinders but does not prevent red mud up-cycling: multiple attempts to transform it into useful products have been reported.[1–10] Those based on vitrification treatment are generally favored in terms of stabilization of pollutants,[3–6] but some sustainability issues remain.

In the management of highly hazardous waste, such as nuclear waste, vitrification is uncontested.[11] The obtainment

of chemically stable wasteforms is a fundamental objective, with absolute priority over costs and energy consumption. For other forms of inorganic waste, on the contrary, sustainability generally depends on a delicate cost/benefits balance: waste-derived glasses should not be simply landfilled, but provide an extra revenue, as raw materials for high-value products, interesting for both mechanical and functional properties.[11] Such cost/benefits balance is further complicated by the necessity of a second heat treatment, for the conversion of waste-derived glasses into new products, such as glass foams or porous and dense glass-ceramics.[11] Besides additional costs, this second treatment implies difficulties in the stabilization of pollutants, for example when a waste-derived glass undergoes crystallization, since pollutants may distribute in both crystal phases and residual glass phase, generally with different chemical composition and durability.[12]

In this paper, we present the results of preliminary studies on the reuse of waste-derived glasses not requiring an energy-intensive transformation. More precisely, we discuss the preparation of cementitious materials for the building industry, with a good stabilization of pollutants, from materials developed following two distinct vitrification strategies.

According to the first approach, a glass was developed by melting a mixture of red mud—as a minor component—with other inorganic waste, including fly ash from coal combustion and glass from discarded pharmaceutical vials (known to be practically unrecyclable).[11] The mixing was designed to determine a material having the proportions between characteristic oxides (alkali oxides, CaO, $Al_2O_3$, and $SiO_2$) approaching those of reactive alumino-silicate glasses, sensitive to activation by NaOH aqueous solution, and thus prone to develop stable "geopolymer-like" gels.[13–15] These reference glasses are known to yield inorganic polymers, by partial dissolution in an alkaline environment and subsequent condensation of hydrated compounds (produced by the same dissolution reactions), and having some fundamental analogies with geopolymers.

Geopolymers are a subgroup of inorganic polymers consisting of "zeolite-like gels," with a characteristic disordered, three-dimensional network structure, determined by the bridging of $[SiO_4]$ and $[AlO_4]$ units—the latter being stabilized by the presence of alkali ions—deriving from various alumino-silicate feedstocks.[16] Formulations relying on Na-based compounds, as an example, correspond to highly durable N–A–S–H (sodium alumino-silicate hydrate) gels.[15] Reactive glasses, according to the presence of CaO, may form C–A–S–H (calcium alumino-silicate hydrate) gels or even mixed gels, that is, (N,C)–A–S–H gels.[13–15] Compared to conventional feedstocks for geopolymers (e.g., natural and waste-derived alumino-silicates), reactive glasses offer more uniform chemical, physical and mineralogical characteristics and may be activated just by simple alkali hydroxide solutions, of limited molarity (<10 M), instead of more aggressive solutions comprising also synthetic compounds, such as alkali silicates.[16]

In the second vitrification approach, a glass was obtained through an "integrated process," consisting of the electric arc furnace (EAF) treatment of a red mud-richer mixture, undergoing carbothermal reduction,[17–19] and yielding a glassy slag as a by-product of iron alloy extraction. As pointed out by Gomez et al.,[11,20] a modern vitrification process is not encouraged commercially only by the transformation of waste-derived glass; extra revenues may be derived from the extraction of combustible gas and/or metals from the same thermal waste treatment. Such operations represent an extension of traditional pyrometallurgical processes, often termed as "smelting," typically enabling the obtainment of a metallic liquid accompanied by a nonmetallic "slag" (generally floating on the metallic bath), separated in form of amorphous or semicrystalline material, depending on the fluxing and cooling conditions.[18] In the present case, the mixing of red mud with CaO had an interesting synergistic effect, enabling both a substantial metal recovery and the development of a stable gel by direct activation with pure water.

## 2 | EXPERIMENTAL PROCEDURE

### 2.1 | Waste-derived glass from conventional melting (CMG)

Red mud (RM1, provided by Alteo, Gardanne, France) was mixed with coal combustion fly ash (FA, Public Power Industry of Greece, Megalopolis, Greece) and pharmaceutical boro-alumino-silicate glass (BSG, courtesy of Nuova OMPI, Padova, Italy). These materials (chemical composition is summarized in Table 1) were mixed with sodium carbonate ($Na_2CO_3$, analytical grade; Sigma Aldrich), in the weight proportions RM1/FA/BSG/$Na_2CO_3$ = 18/58/13/11 and melted at 1500°C for 2 h, in a platinum crucible, using superkanthal ($MoSi_2$) furnace. After treatment, the melt was poured on cold steel plates producing opaque slabs (Figure 1). The chemical composition, determined by X-ray fluorescence (XRF), is reported in Table 1.

The material, after cooling, was first hand crushed and then dry ball milled (Pulverisette 6; Fritsch GmbH), to obtain fine powders (<75 μm). The powders were finally activated by casting in alkaline solution (8 M NaOH), included in cylindrical polystyrene containers, at 70–30 weight solid–liquid ratio, and mechanically stirred (300 rpm) for 10 min. The suspensions were then leveled out, the containers were covered by a lid and kept for 7 days at 40°C.

### 2.2 | Waste-derived glass from electric arc furnace processing and carbothermal reduction (EAG)

A second batch of the red mud (RM2 obtained from Aluminium of Greece SA, see Table 1) was dried for 24 h at

**TABLE 1** Material from conventional melting of red mud containing waste mixture and cooling on steel plate

| | Red mud (RM1) | Fly Ash (FA) | Pharmaceutical glass (BSG) | Material from conventional melting (CMG) | Red mud (RM2) | Material from electric arc furnace (EAG) smelting |
|---|---|---|---|---|---|---|
| $SiO_2$ | 5.2 | 49.4 | 72.0 | 45.2 | 6.2 | 9.9 |
| $Al_2O_3$ | 15 | 22.7 | 7.0 | 19.5 | 25.3 | 29.2 |
| $Fe_2O_3$ | 52.9 | 7.4 | — | 15.3 | 44.3 | 2.3 |
| $Na_2O$ | 2.4 | 0.9 | 6.0 | 8.5 | 2.0 | 2.6 |
| $K_2O$ | 0.6 | 1.4 | 2.0 | 2.3 | | |
| CaO | 11.7 | 8.9 | 1.0 | 4.0 | 8.5 | 44.5 |
| MgO | 0.6 | 2.0 | — | 1.4 | 0.3 | 0.7 |
| $B_2O_3$ | — | — | 12.0 | 1.2 | | |
| $TiO_2$ | — | — | — | — | 5.2 | 9.0 |
| Others | 5.1 | 6.1 | — | 4.1 | 8.2 | 1.8 |

100°C. Lime in excess of 20% and lignite coke (87% carbon content), at a ratio of 1:10, were used in combination with red mud to carbothermally reduce the iron oxides into metallic iron, by heating in a lab-scale EAF (see Figure 2) operating in single-phase DC mode. The equipment utilized a graphite rod 50 mm in diameter as a top electrode, and a graphite crucible of 150 mm in diameter and 220 mm height to carry up to 2.5 kg of material serving as a counter-electrode. The power was varied between 2.5 and 10 kW to maintain a temperature of around 1500–1550°C in the furnace. Carbothermic reduction consisted of 20 min of charging and one hour of holding time. After the thermal treatment, the molten liquid comprising of slag and metal was either quenched in water (Figure 3a) or tapped out into a casting ladle (Figure 3b), and in both cases the slag and metal separated with ease.

A glassy slag obtained by water quenching (composition shown in Table 1) was hand crushed and dry ball milled, to obtained fine powders (<75 μm). The powders were activated by mixing them with deionized water in a polystyrene container at a 35–65 solid–liquid weight ratio. Hand-mixing for 10 min resulted in a considerable thickening of the mixture. The suspension was then leveled out, the container was covered by a lid and kept for 7 days at 40°C. To improve the leaching resistance in aqueous media, an additional set of samples was prepared with 30wt% of glass replaced by the common soda-lime-silica glass (<30 μm fraction, courtesy of SASIL S.p.A., Biella, Italy).


**FIGURE 1** Material from conventional melting of red mud containing waste mixture and cooling on steel plate

## 2.3 | Characterization of binders

"Activated" waste-derived glasses were subjected to a preliminary stability test. Monolithic pieces (4 g each) of glass were boiled in 500 ml of deionized water for 30 min, to assess possible dissolution or cracking.

In a subsequent step, the samples were subjected to infrared spectroscopy (FTIR 2000; Perkin Elmer), mineralogical analysis (XRD; Bruker D8 Advance, Karlsruhe Germany-CuKα radiation 0.15418 nm), helium pycnometry (Micromeritics AccuPyc 1330), and scanning electron microscopy (SEM FEI Quanta 200 ESEM). The phase identification from X-ray diffraction patterns was performed with the use of HighScore Plus (v. 3.0.4; PANalytical B.V.) supported by the PDF4+ 2014 database.

Representative samples of approximately 3 mm × 4 mm × 40 mm were cut from bulk specimens and subjected to three-point flexural tests (Quasar 25; Galdabini), operating at a crosshead speed of 1 mm $min^{-1}$. At the same time, the samples were also cut into approximately 5 mm × 5 mm × 5 mm cubic blocks, which were subjected to a compression test. Each data point is the average of five independent measurements.

To assess the chemical stability of prepared samples, 1 g of crushed sample total (pieces were smaller than 10 mm) was placed into a polypropylene test tube with 10 g of deionized water, to obtain a solid/liquid ratio of 1/10 w/w. The suspensions were stirred for 24 h, after which clear solutions were obtained via decantation, centrifuging, and filtering.

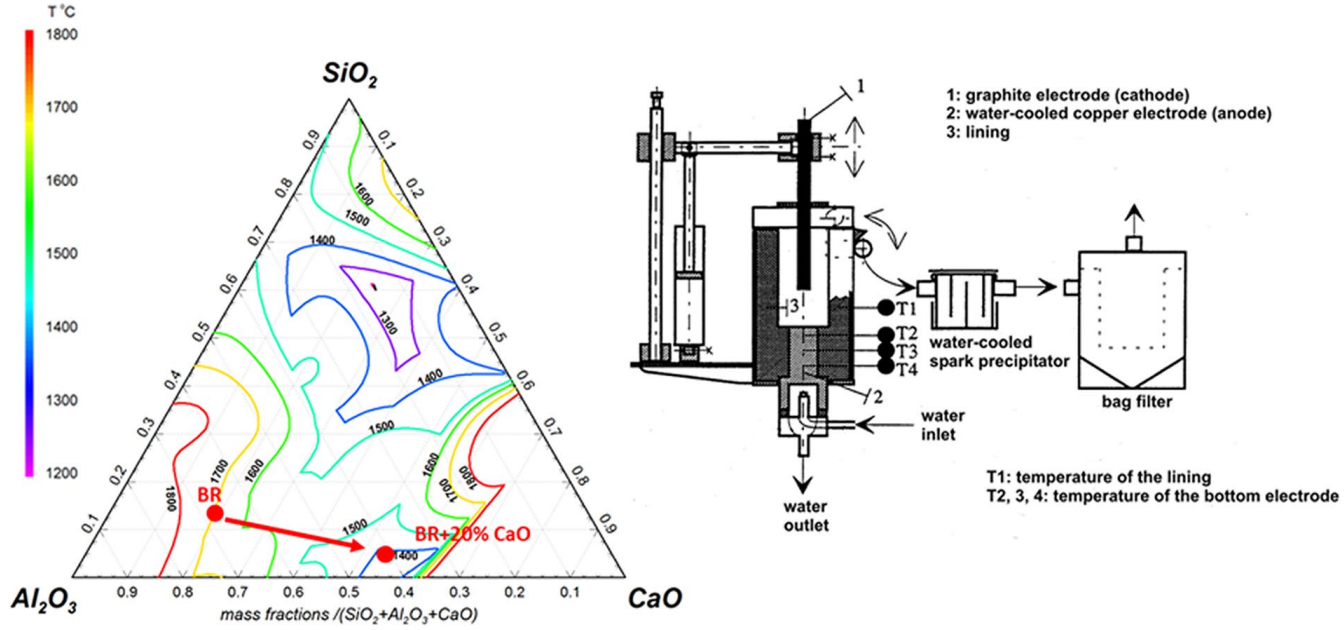


**FIGURE 2** Left: Ternary phase diagram, as predicted by FactSage 6.4, for $SiO_2$–$Al_2O_3$–CaO–4%$Na_2O$–8.5%$TiO_2$ detailing the temperatures of formation of the liquid slag; right: scheme of Lab-scale DC EAF

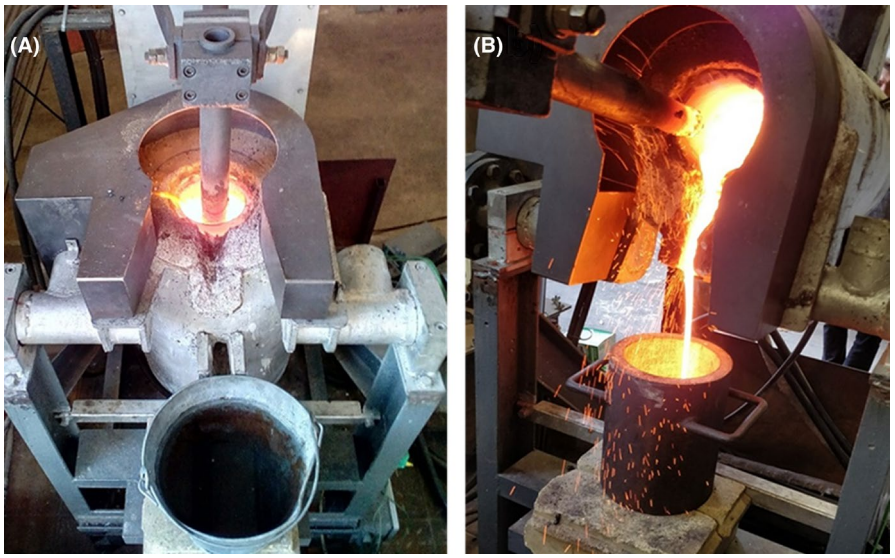


**FIGURE 3** DC-EAF operation: (A) quench in water; (B) tapping into casting ladle

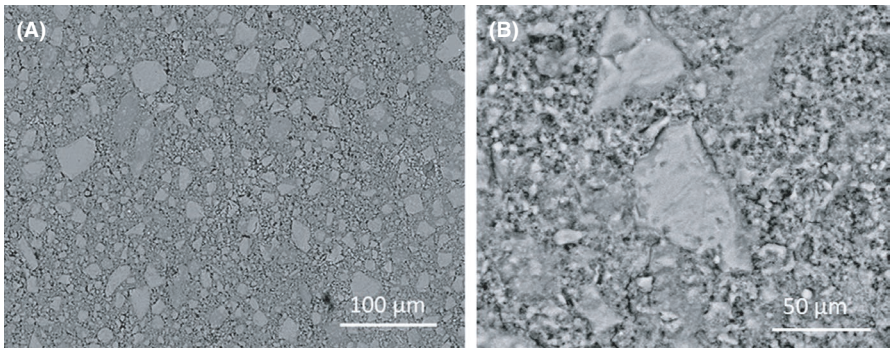


**FIGURE 4** SEM micrographs of activated CMG: overall view (A), larger magnification detail of individual CMG particles surrounded by porous gel matrix (B)

Leachates were analyzed via optical emission spectroscopy in inductively coupled plasma (ICP-OES, Agilent 7500 cx).

## 3 | RESULTS

### 3.1 | Activation of CMG

A preliminary assessment of the stability of prepared gels was carried out by boiling test. No disintegration or dissolution was observed. The microstructure of hardened samples was homogeneous, consisting of a microporous gel (binder) connecting unreacted, irregularly shaped glass particles of CMG (Figure 4A). The higher magnification detail in Figure 4B confirms the porosity of the gel surrounding CMG particles.

The gelation was studied by X-ray diffraction analysis. The starting material was not completely amorphous, since some separation of magnetite ($Fe_3O_4$, PDF #82-1533) occurred upon cooling of the melt (Figure 5). However, this did not affect the expected reaction with the alkaline solution. The results shown in Figure 5 confirmed that, after activation and curing (for 7 days), the material was transformed: this was documented by the shift of the background hump to higher $2\theta$ angles and the appearance of new, weak diffraction lines.

The new diffraction maxima are consistent with the formation of zeolite phases, that is, sodium aluminum silicate hydrate (zeolite Y, $Na_{1.84}Al_2Si_4O_{11.92}{\cdot}7H_2O$, PDF#38-0238) and calcium aluminum silicate hydrate (cowlesite, $CaAl_2Si_3O_{10}{\cdot}6H_2O$, PDF#46-1405).

Infrared spectroscopy provided further structural information (Figure 6). The typical absorption bands of zeolites

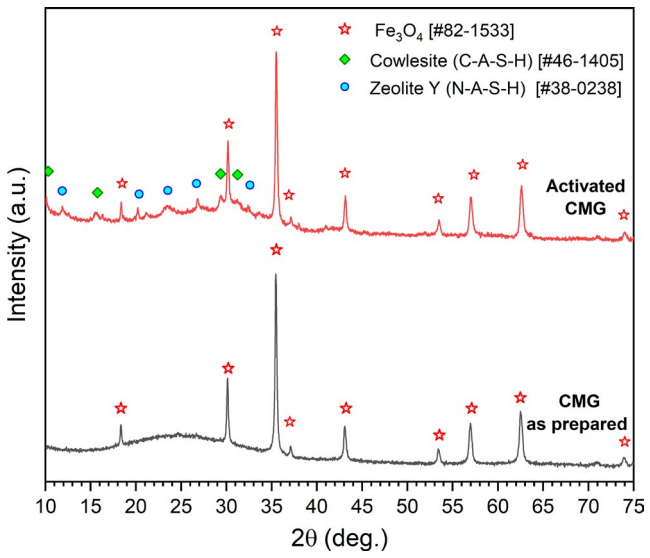


**FIGURE 5** X-ray diffraction analysis of CMG before and after alkali activation

(namely from an asymmetric and symmetric stretch of T–O bonds, corresponding to oxygen connected with Al or Si ions in tetrahedral coordination) were distinguished in the spectrum of activated material.[21] Minor bands corresponded to hydrated carbonated compounds (for analogous alkali-activated glasses Garcia-Lodeiro et al.[14] suggested the formation of amorphous hydrated sodium carbonate), magnetite (at 600 and 470 $cm^{-1}$)[22] and -OH functionalities in the same zeolite structure.[23] Well-distinguished peaks corresponded to $CO_2$ absorbed from the atmosphere, as already observed for pure Na zeolites.[24]

Table 2 shows that the RG-derived material possessed a complex of physical and mechanical properties (with the exception of the elastic modulus) comparing well with those of "lightweight concrete" (data extracted from the Cambridge Engineering Selector database).[25] It should be noted, however, that CMG-derived material was not concrete, that is, it did not contain aggregates, which contributed to mechanical properties.

Despite the fact the CMG was not a homogeneous glass, leaching tests confirmed that the release of ions was well below the limits for inert materials (according to European regulations).[12] The stabilization of pollutants was less effective in the material obtained after alkali activation. The levels of released ions were still far below the limits for non-hazardous materials, but the contents of As and Mo were slightly higher than the thresholds for inert materials.

### 3.2 | Activation of EAG

The carbothermal reduction in EAF resulted in a dramatic reduction in the iron content in the nonmetallic fraction, floating on the molten metal bath, from the processed red mud (Table 1). Despite the low $SiO_2$ content, this nonmetallic liquid transformed into an almost amorphous material (EAG) after quenching in water. The weak diffraction maxima in the diffraction pattern shown in Figure 7, could be attributed to α-quartz ($SiO_2$, PDF#88-2487), gehlenite ($Ca_2Al_2SiO_7$, that is, $2CaO{\cdot}Al_2O_3{\cdot}SiO_2$, PDF#74-1607), and perovskite ($CaTiO_3$, PDF#82-0228).

Due to its silica-poor calcium alumino-silicate formulation, EAG was not activated in alkaline solution: gelation could be achieved by interaction with pure water. Despite the much different formulation, the EAG-derived material did not show any dissolution or degradation after immersion in boiling water. A detail of the cementitious material developed upon hardening of suspensions is shown in Figure 8a. The structure is quite homogenous, with small un-reacted particles surrounded by a gel matrix. According to EDX analysis (not shown), black spots were identified as residual carbon particles from the reduction reaction, whereas the bright spots in the structure were Ti and Ca-rich and were identified as the perovskite phase.

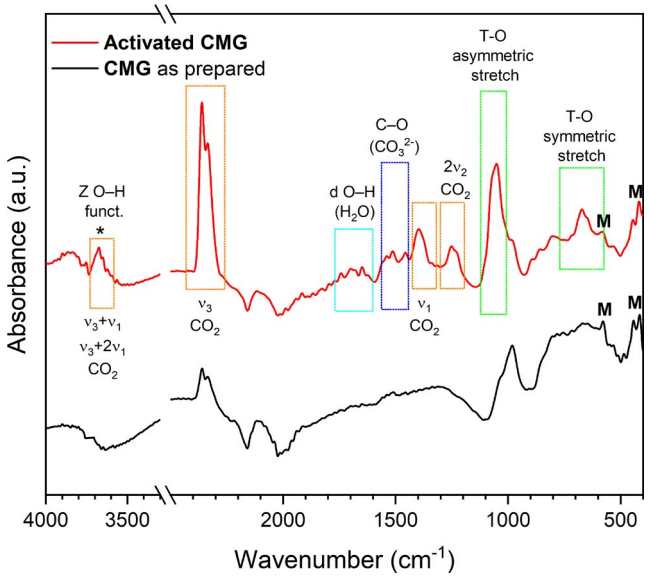


FIGURE 6 Infrared spectra of CMG before and after alkali activation

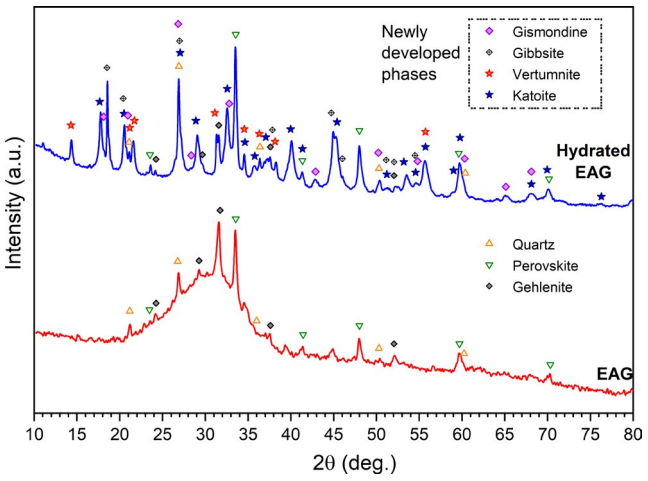


FIGURE 7 XRD pattern of EAG, in the as received state and after curing for 7 days

Despite the absence of any alkaline activator, the reaction between glass and water was remarkable, and well visible directly from the results of X-ray diffraction analysis (Figure 7). A multitude of crystalline reaction products was formed, corresponding to hydrated compounds. The anhydrous phases originally embedded in glass, such as perovskite and gehlenite, were still detected, but with significant differences. Considering the practically unaltered intensity of related diffraction maxima, perovskite could be considered an inert phase. The intensities of gehlenite diffraction maxima were much reduced, indicating reaction with water. A clear identification of quartz was not possible, due to the presence of newly formed phases with overlapping diffraction lines.

The newly formed crystalline phases comprised katoite ($Ca_{2.93}Al_{1.97}(Si_{0.64}O_{2.56})(OH)_{9.44}$, PDF#77-1713), and vertumnite ($Ca_4Al_2(Si_{2.89}Al_{2.23}O_{5.18}(OH)_{21.88})(H_2O)_{4.38}$, PDF#83-1522). Katoite is a silica-poor, highly hydrated variant of hydrogrossular (described by the general formula $Ca_3Al_2(SiO_4)_{3-x}(OH)_{4x}$),[26] consistent with the high CaO and $Al_2O_3$ contents in the glass. Vertumnite is structurally very similar to strätlingite, also known as "hydrated gehlenite," and it can be seen as proof of gehlenite reaction. Traces of gismondine ($CaAl_2Si_2O_8{\cdot}4H_2O$), that is, a Ca-based zeolite,[27] and aluminum hydroxide ($Al(OH)_3$, gibbsite, PDF#74-1775) were also detected.

By itself, EAG did not provide an optimum stabilization of pollutants, as shown in Table 3. It could be considered as nonhazardous, but the release of some elements (Cd, Pb, Se) was above the threshold for inert materials. The hydration reaction stabilized these elements, with leachates falling

TABLE 2 Density and mechanical properties of CMG- and EAG-derived materials

| | CMG | EAG | | |
|---|---|---|---|---|
| | Activated | As prepared | With SLG filler | Lightweight concrete |
| Density $\rho$ (g/cm$^3$) | 1.75 ± 0.11 | 1.59 ± 0.05 | 1.74 ± 0.16 | 1.4–2 |
| Closed porosity (vol%) | 8.5 | 1.9 | 1.3 | |
| Open porosity (vol%) | 14.3 | 21.4 | 22.2 | |
| Total porosity (vol%) | 21.8 | 23.3 | 23.5 | |
| Elastic modulus $E$ (GPa) | 7.9 ± 0.4 | 5.4 ± 0.6 | 5.0 ± 0.6 | 11–21 |
| Bending strength $\sigma_b$ (MPa) | 8.1 ± 0.7 | 6.0 ± 0.4 | 4.1 ± 0.6 | 3–17 |
| Crushing strength $\sigma_c$ (MPa) | 11.6 ± 1.6 | 7.3 ± 0.8 | 5.8 ± 0.7 | 11–28 |

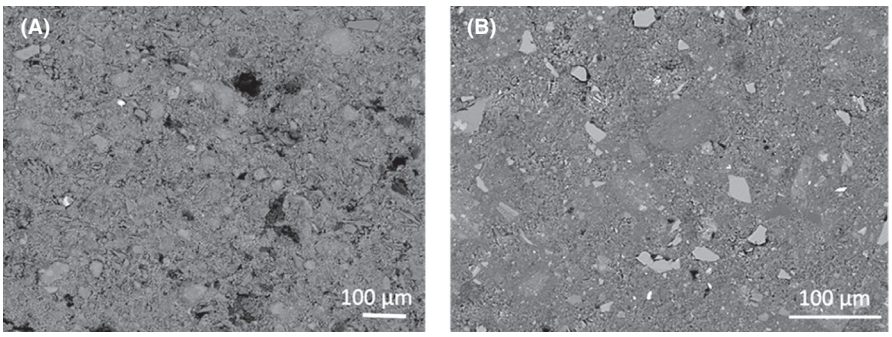


**FIGURE 8** Micrographs of gel from hydration of EAG, without (A) and with (B) soda-lime glass filler

slightly below the thresholds from inert materials; however, Cr and Sb releases, quite surprisingly, were enhanced.

The inclusion of fine recycled soda-lime glass powder led to a "mortar" (Figure 8B), after hydration and drying, still surviving the boiling test. The composite effectively met the conditions for complete immobilization of pollutants, as shown in Table 3. Finally, as reported in Table 2, both materials from pure EAG and EAG mixed with SLG compared well with lightweight concrete in terms of density and bending strength. Further optimizations, with different additives (also to be selected in terms of granulometry), will be the object of future work.

## 4 | DISCUSSION

### 4.1 | CMG-based materials

CMG was prepared and studied with two main objectives: (i) stabilization of different wastes by the creation of a chemically stable material; (ii) exploitation of the waste-derived material as a constituent of a geopolymer-like binder. Reports on the stabilization of inorganic waste, such as red mud and coal combustion fly ash by direct alkali activation and development of inorganic polymers—that is, stable gels with zeolite-like three-dimensional network structure or similar (comprising geopolymers)—are abundant,[8–10,28] but several issues still need to be addressed. First, national and regional regulations may complicate the transportation of inorganic waste—especially if they contain heavy metals—from the production/storage site to the place where the waste-derived inorganic polymer is manufactured. On the contrary, an "inert" material is easily transported. Second, inorganic polymers are generally obtained from condensation reactions at nearly room temperature, involving the products of the dissolution of wastes—replacing valuable alumino-silicate natural raw materials—in aqueous solutions of complex formulation, that is, not comprising just alkali hydroxides, but involving also synthetic alkali silicates and aluminates.[28,29] Finally, when using wastes, the formulations must be continuously adjusted, reflecting their variability.

CMG was designed to mimic a specific range of alumino-silicate glasses, undergoing alkali activation and thus

**TABLE 3** Results of the leaching tests performed on starting glassy materials and on materials after hardening

| | Leachates [ppm] | | | | | | |
|---|---|---|---|---|---|---|---|
| Element | Limits for not hazardous | Limits for inert | CMG | Activated CMG | EAG | Hydrated EAG | Hydrated EAG/SLG |
| As | **2** | **0.5** | <0.018 | **0.638** | <0.018 | 0.030 | <0.018 |
| Ba | **100** | **20** | <0.140 | <0.140 | <0.140 | <0.140 | <0.140 |
| Cd | **1** | **0.04** | <0.013 | <0.013 | **0.061** | **0.037** | <0.013 |
| Cr | **10** | **0.5** | 0.0290 | <0.013 | <0.013 | **1.100** | <0.013 |
| Cu | **50** | **2** | <0.012 | <0.012 | <0.012 | 0.03 | <0.012 |
| Mo | **10** | **0.5** | <0.013 | **0.634** | <0.013 | 0.060 | <0.013 |
| Ni | **10** | **0.4** | <0.012 | <0.012 | <0.012 | <0.012 | <0.012 |
| Pb | **10** | **0.5** | 0.014 | 0.068 | **0.663** | <0.010 | <0.010 |
| Sb | **0.7** | **0.06** | <0.013 | <0.013 | <0.013 | **0.320** | <0.013 |
| Se | **0.5** | **0.1** | <0.012 | 0.0500 | **0.118** | 0.080 | <0.012 |
| Zn | **50** | **4** | <0.014 | <0.014 | <0.014 | <0.014 | <0.014 |

providing new forms of cementitious materials.[13–15] The $SiO_2$/$Al_2O_3$ balance was kept close to the references by the mixing of red mud with fly ash. The CaO content was "diluted" by considering a CaO-poor, boro-alumino-silicate pharmaceutical glass, as an additional constituent. The content of CaO was decreased with the aim to avoid the formation of not very stable tobermorite-like gels (C–S–H, i.e., calcium silicate hydrate), typically found in hydration products of conventional cements.[16] The addition of pharmaceutical glass had important additional advantages:

1. the softening of a glass constituent in a glass-forming batch typically catalyzes the dissolution of other components[11];
2. pharmaceutical glass is practically unrecyclable, that is, cullet cannot be reused in the manufacturing of the original articles, due to risks of contamination and practical limitations (highly chemically stable vials are typically manufactured by thermomechanical processing of glass tubes, produced elsewhere); an unrecyclable glass represents, by itself, a form of inorganic waste[11];
3. $Al_2O_3$ and $B_2O_3$ are known to enhance the durability of glasses, by stabilizing alkali ions, forming [$AlO_4$] and [$BO_4$] units[11];
4. in terms of alkali activation and subsequent gelation, the [$AlO_4$] and [$BO_4$] units combine with [$SiO_4$] units, yielding zeolite-like gels.[30]

Operating with a waste mixture, instead of focusing on red mud, the composition of CMG was kept quite constant. This approach eliminated variations in the chemical composition of red mud and other constituents. In other words, the approach to CMG was analogous with that applied to waste-derived glasses converted into glass-ceramics (the crystallization and the properties of the products are quite predictable only referring to quite specified compositions).[6,11]

Despite the reduction in red mud as the waste featuring the highest iron content, the content of iron oxide remained substantial, and well above the iron levels in reference glasses. Some separation of iron oxide-based phases was therefore expected upon cooling from the melt, as usually observed in Fe-rich glasses.[31]

The main objectives of CMG processing were achieved. The separation of magnetite did not compromise the stabilization of pollutants, most likely due to the presence of $Al_2O_3$ and $B_2O_3$ in the glass matrix. The iron oxide content could even increase the value of the material in the building industry, adding extra functionalities offered by dispersed magnetic particles, such as electromagnetic shielding.[32]

The activation of CMG led to the formation of a semicrystalline gel (see Figure 5) with important analogies and differences with those provided by reference glasses. The stability of the gel was confirmed by the boiling test. Although qualitative, such a test is particularly severe, since it may result in swelling or total destruction of nonfully condensed geopolymeric materials.[33]

Similar to reference glasses, a shift of the hump centered in the X-ray diffraction pattern of anhydrous glass at $2\theta = 20–40°$, to higher $2\theta$ values, could be ascribed to precipitation of an N–A–S–H-type gel.[14] The formation of zeolite crystal inclusions could be also seen as a common feature with the reference glasses, despite important differences in the chemical composition. Garcia Loderio et al. reported the development of sodium alumino-silicate hydrate zeolites (analogous to N–A–S–H gel), with a fraction of calcium ions involved in the precipitation of other crystalline compounds, such as portlandite ($Ca(OH)_2$).[14] In the present case, calcium was included just in one of the two zeolite phases (cowlesite). The presence of zeolites justified the observed $CO_2$ absorption (Figure 6) which, coupled with magnetite (widely recognized catalyst), may constitute the basis for additional functional applications (e.g., conversion of carbon dioxide as fuel).[34]

The binding phase developed around unreacted CMG particles could not immobilize all metal ions, similarly to geopolymers from direct activation of red mud-containing mixtures.[35] This issue is not seen as particularly substantial, since the developed cementitious system could be applied by itself as a binder for new mortars and concretes, involving inert aggregates. The leaching from the CMG-derived gel would be then reduced, due to the dilution of CMG with secondary materials. Studies on mortars, along with the refined characterization of the gels, will constitute the focus of future investigations. These will also include studies on the mechanical properties of much larger samples. The observed limited mechanical properties could have been negatively affected by microcracks induced upon machining of test samples.

## 4.2 | EAG-derived materials

EAG was the result of a pyrometallurgical process which is, unlike conventional vitrification, applicable to red mud as a dominant component. The process involved a red mud sample (RM2) of a different composition from that used in CMG development (RM1). However, some "tuning" possibilities are applicable in both technologies. While in conventional vitrification compositional variations of the constituents may be compensated by adjusting the proportion between them, in EAF processing, the production of pig iron by carbothermal reduction is accompanied by the conditioning of slag properties through the addition of fluxes such as lime, quartz, or even other mineral wastes.[17–19,36–38] Other types of inorganic waste (i.e., fly ash) might be co-reduced alongside red mud. The process successfully manages to extract

up to 90% of Fe and 98% of other heavy metals, especially Cd and Pb. The residual nonmetallic slag fraction consists mostly of CaO, $Al_2O_3$, and $SiO_2$ and contains a substantially lower amount of pollutants, which is advantageous for its further reprocessing.[19]Furthermore, conditioning of slag is also achievable through cooling rates, where fast cooling promotes the transformation of a liquid slag into an amorphous material while slow cooling favors the formation of a more crystalline material.

EAG was derived from a preliminary study of the $SiO_2$–$Al_2O_3$–CaO–8.5%$TiO_2$ ternary diagram detailing the temperature of formation of the liquid phase, between 1200 and 1800°C, computed using FactSage 6.4 (Facility for the Analysis of Chemical Thermodynamics) program package. As illustrated by Figure 2, the addition of lime was intended to reduce the processing temperature, but affected also the chemistry of EAG. Despite the low $SiO_2$ content, the nonmetallic liquid transformed into an almost amorphous material (EAG) after quenching in water.

Owing to this particular formulation, EAG could be considered as a calcium aluminate glass. In crystallized form, alone or mixed with other compounds (e.g., calcium silicates), calcium aluminates are well-known components of traditional types of cement.[39] Unlike silicates, such as β-$2CaO{\cdot}SiO_2$ and $3CaO{\cdot}SiO_2$, calcium aluminates typically exhibit direct and rapid hydration without the formation of $Ca(OH)_2$ as a by-product. These reactions are exploited for short-term hardening of mortars and concretes.[39] The prevalently amorphous nature of EAG further promoted its reactivity.

The presence of traces of gehlenite, as a crystal phase embedded in EAG, was interesting, since it is a reference for calcium alumino-silicate glass cements.[40] Glasses of gehlenite stoichiometry react with water easily and form cementitious phases, such as "strätlingite," that is, hexagonal hydrated gehlenite ($Ca_2Al_2SiO_7{\cdot}10H_2O$).[41] The phase belongs to the vast group of hydrated calcium alumino-silicate (C–A–S–H) compounds found in ancient mortars and featuring excellent durability.[42]

Gehlenite glasses were subjected to intensive research nearly three decades ago, as fast-setting materials for rapid road reconstruction in the U.S.[43] To the best authors' knowledge, these glasses have no current commercial exploitation, probably due to the high temperatures required for their melting.[43] It should be noted, however, that gehlenite may react—yielding strätlingite—also in form of nanocrystals.[44]

The direct, rapid reaction of EAG with water was consistent with the observations reported above. Upon hydration, EAG likely yielded a cementitious material analogous to those produced by many modern alkali-activated slag (AAS) binders, featuring a C–A–S–H gel (generally including also sodium), and embedding crystalline phases such as katoite, strätlingite, and gismondine zeolite.[45] C–A–S–H gels are typically more stable than tobermorite-like gel (calcium silicate hydrate, C–S–H), due to the cross-linking of calcium silicate chains operated by [$AlO_4$] units, which replace [$SiO_4$] units in the structure of the gel.[45] Such interconnected molecular structure would justify the resistance of EAG-derived samples to water boiling test and the enhanced stabilization of pollutants (hydrated EAG led to lower leaching than as prepared EAG). Refined studies on the gel will constitute an additional objective of further investigations, but the activation without alkali is undoubtedly promising in the perspective of facile upcycling of inorganic waste. Also in the case of EAG-derived materials, the mechanical properties should be studied on much larger samples, to eliminate any negative effect of sample machining.

## 5 | CONCLUSIONS

Waste-derived glasses from critical industrial residues, mainly consisting of red mud from the refining of Al-rich ores, were found to represent new precursors for inorganic binders. After activation with an alkaline solution of limited molarity (8 M NaOH) or even with pure water, these glasses can be applied as promising building materials. Both conventional vitrification and EAF processing, combined with carbothermal reduction and water quenching, allowed for modulation of chemical composition, reflected in the changes of calcium and iron content of the related glassy products. Conventional vitrification relied on the combination of waste to reduce CaO and $Fe_2O_3$, and to obtain an almost amorphous alumino-silicate material prone to transformation into a geopolymer-like binder. The carbothermal reduction provided an additional opportunity for more direct treatment of red mud, implying a dramatic decrease in overall iron content separated in form of metal alloy. Owing to the concentration of $Al_2O_3$ and CaO as well as the almost amorphous nature mainly attributed to water quenching, the nonmetallic residue exhibited an impressive reactivity, producing a stable binder activated by the addition of water. Composition refinements and additional studies, especially concerning mechanical properties, are still necessary, but the reported approaches may support the extensive upcycling of inorganic waste in a new generation of glass-based construction materials. The main advantages comprise simultaneous treatment of different waste by conventional melting and the extra revenues from metal separation by EAF processing.

### ACKNOWLEDGMENTS

This paper is a part of the dissemination activities of project "FunGlass" (Centre for Functional and Surface Functionalized Glass). This project has received funding from the European Union's Horizon 2020 research and innovation program under grant agreement no. 739566. The authors also gratefully acknowledge the financial support from the Slovak

Grant Agency of Ministry of Education, Science, Research and Sport, VEGA Nr 2/0091/20. Enrico Bernardo and Bernd Friedrich acknowledge also the funding by the European Union's Horizon 2020 research and innovation program, under the Marie Skłodowska-Curie project "NEW-MINE" (EU Training Network for Resource Recovery through Enhanced Landfill Mining), grant agreement no. 721185. Enrico Bernardo acknowledges the additional funding from the University of Padova (Dept. of Industrial Engineering), in the framework of the "SusPIRe" (Sustainable porous ceramics from inorganic residues, BIRD202134). Enrico Bernardo thanks Prof. Yiannis Pontikes (KU Leuven, Belgium) for supplying coal combustion FA.

## ORCID

*Miroslava Hujova* https://orcid.org/0000-0003-0876-7292
*Patricia Rabelo Monich* https://orcid.org/0000-0003-0436-8091
*Dusan Galusek* https://orcid.org/0000-0001-5995-8780
*Enrico Bernardo* https://orcid.org/0000-0003-4934-4405

## REFERENCES

1. Joseph CG, Taufiq-Yap YH, Krishnan V, Puma GL, Joseph CG. Application of modified red mud in environmentally-benign applications: a review paper. Environ Eng Res. 2020;25(6):795-806. https://doi.org/10.4491/eer.2019.374
2. Mukiza E, Zhang LingLing, Liu X, Zhang NA. Resources, conservation & recycling utilization of red mud in road base and subgrade materials: a review. Res Cons Recycl. 2019;2018(141):187–99. https://doi.org/10.1016/j.resconrec.2018.10.031
3. Park HS, Park JH. Vitrification of red mud with mine wastes through melting and granulation process – preparation of glass ball. J Non-Cryst Sol. 2017;475:129–35. https://doi.org/10.1016/j.jnoncrysol.2017.09.010
4. Liu T, Zhang J, Wu J, Liu J, Li C, Ning T, et al. The utilization of electrical insulators waste and red mud for fabrication of partially vitrified ceramic materials with high porosity and high strength. J Clean Prod. 2019;223:790–800. https://doi.org/10.1016/j.jclepro.2019.03.162
5. Peng F, Liang K, Shao H, Hu A. Nano-crystal glass-ceramics obtained by crystallization of vitrified red mud. Chemosph. 2005;59:899–903. https://doi.org/10.1016/j.chemosphere.2004.11.002
6. Bernardo E, Esposito L, Rambaldi E, Tucci A, Pontikes Y, Angelopoulos GN. Sintered esseneite-wollastonite-plagioclase glass-ceramics from vitrified waste. J Eur Ceram Soc. 2009;29(14):2921–7. https://doi.org/10.1016/j.jeurceramsoc.2009.05.017
7. Kim S, Yang D, Rao SV, Nam C, Rhee K, Sohn J. A new approach to the recycling of gold mine tailings using red mud and waste limestone as melting fluxes. Geosyst Eng. 2012;15(1):44–9. https://doi.org/10.1080/12269328.2012.674683
8. He J, Zhang J, Yu Y, Zhang G. The strength and microstructure of two geopolymers derived from metakaolin and red mud-fly ash admixture: a comparative study. Constr Build Mat. 2012;30:80–91. https://doi.org/10.1016/j.conbuildmat.2011.12.011
9. Hajjaji W, Andrejkovičová S, Zanelli C, Alshaaer M, Dondi M, Labrincha JA, et al. Composition and technological properties of geopolymers based on metakaolin and red mud. J Clean Prod. 2013;52:648–54. https://doi.org/10.1016/j.matdes.2013.05.058
10. Badanoiu AI, Al Saadi THAA, Stoleriu S, Voicu G. Preparation and characterization of foamed geopolymers from waste glass and red mud. Constr Build Mat. 2015;84:284–93. https://doi.org/10.1016/j.conbuildmat.2015.03.004
11. Rincón Romero A, Marangoni M, Cetin S, Bernardo E. Recycling of inorganic waste in monolithic and cellular glass-based materials for structural and functional applications. J Chem Tech Biotech. 2016;91:1946–61. https://doi.org/10.1002/jctb.4982
12. Rabelo Monich P, Rincón Romero A, Höllen D, Bernardo E. Porous glass-ceramics from alkali activation and sinter-crystallization of mixtures of waste glass and residues from plasma processing of municipal solid waste. J Clean Prod. 2018;188:871–8. https://doi.org/10.1016/j.jclepro.2018.03.167
13. Garcia-Lodeiro I, Fernández-Jimenez A, Pena P, Palomo A. Alkaline activation of synthetic aluminosilicate glass. Ceram Int. 2014;40(4):5547–58. https://doi.org/10.1016/j.ceramint.2013.10.146
14. Garcia-Lodeiro I, Aparicio-Rebollo E, Fernández-Jimenez A, Palomo A. Effect of calcium on the alkaline activation of aluminosilicate glass. Ceram Int. 2016;42(6):7697–707. https://doi.org/10.1016/j.ceramint.2016.01.184
15. Ruiz-Santaquiteria C, Palomo A. Alternative prime materials for developing new cements: alkaline activation of alkali aluminosilicate glasses. Ceram Int. 2016;42(8):9333–40. https://doi.org/10.1016/j.ceramint.2016.03.111
16. Provis JL. Geopolymers and other alkali activated materials: why, how, and what? Mater Struct. 2014;47(1-2):11–25. https://doi.org/10.1617/s11527-013-0211-5
17. Kaußen F, Friedrich B. Reductive smelting of red mud for iron recovery. Chemie Ing Tech. 2015;87(11):1535–42. https://doi.org/10.1002/cite.201500067
18. Valeev D, Zinoveev D, Kondratiev A, Lubyanoi D, Pankratov D. Reductive smelting of neutralized red mud for iron recovery and produced pig iron for heat-resistant castings. Metals. 2019;10(1):32. https://doi.org/10.3390/met10010032
19. Geng C, Chen C, Shi X, Wu S, Jia Y, Du B, et al. Recovery of metals from municipal solid waste incineration fly ash and red mud via a co-reduction process. Res Cons Recycl. 2019;154:104600. https://doi.org/10.1016/j.resconrec.2019.104600
20. Gomez E, Rani DA, Cheeseman CR, Deegan D, Wise M, Boccaccini AR. Thermal plasma technology for the treatment of wastes: a critical review. J Haz Mat. 2009;161:614–46. https://doi.org/10.1016/j.jhazmat.2008.04.017
21. Rodriguez SA. Vibrational spectroscopy and structural analysis of Na–Y zeolite. Vibr Spectr. 1995;9(2):225–8. https://doi.org/10.1016/0924-2031(94)00082-R
22. Morel M, Martínez F, Mosquera E. Synthesis and characterization of magnetite nanoparticles from mineral magnetite. J Magn Magn Mater. 2013;343:76–81. https://doi.org/10.1016/j.jmmm.2013.04.075
23. Khabtou S, Chevreau T, Lavalley JC. Quantitative infrared study of the distinct acidic hydroxyl groups contained in modified Y zeolites. Microporous Mater. 1994;3(1):133–48. https://doi.org/10.1016/0927-6513(94)00015-8
24. Galhotra P, Navea JG, Larsen SC, Grassian VH. Carbon dioxide ($C^{16}O_2$ and $C^{18}O_2$) adsorption in zeolite Y materials:

effect of cation, adsorbed water and particle size. Energy Env Sci. 2009;2(4):401–9. https://doi.org/10.1039/B814908A
25. CES (Cambridge Engineering Selector) EduPack. 2020. https://www.ansys.com/it-it/products/materials/granta-edupack
26. Hôpital EL, Lothenbach B, Le Saout G, Kulik D, Scrivener K. Cement and concrete research incorporation of aluminium in calcium-silicate-hydrates. Cem Concr Res. 2015;75:91–103. https://doi.org/10.1016/j.cemconres.2015.04.007
27. Stone-Weiss N, Youngman RE, Thorpe R, Smith NJ, Pierce EM, Goel A. An insight into the corrosion of alkali aluminoborosilicate glasses in acidic environments. Phys Chem Chem Phys. 2020;22(4):1881–96. https://doi.org/10.1039/C9CP06064B
28. Toniolo N, Boccaccini AR. Fly ash-based geopolymers containing added silicate waste. A review. Ceram Int. 2017;43(17):14545–51. https://doi.org/10.1016/j.ceramint.2017.07.221
29. Brew DRM, MacKenzie KJD. Geopolymer synthesis using silica fume and sodium aluminate. J Mat Sci. 2007;42(11):3990–3. https://doi.org/10.1007/s10853-006-0376-1
30. Taveri G, Tousek J, Bernardo E, Toniolo N, Boccaccini AR, Dlouhy I. Proving the role of boron in the structure of fly-ash/borosilicate glass based geopolymers. Mater Lett. 2017;200:105–8. https://doi.org/10.1016/j.matlet.2017.04.107
31. Francis AA. Magnetic characteristics of iron-containing glass originated from the mixture of various wastes. Ceram Int. 2007;33(2):163–8. https://doi.org/10.1016/j.ceramint.2005.09.005
32. Guan B, Ding D, Wang L, Wu J, Xiong R. The electromagnetic wave absorbing properties of cement-based composites using natural magnetite powders as absorber. Mater Res Expr. 2017;4(5):056103. https://doi.org/10.1088/2053-1591/aa7025
33. Davidovits J. Geopolymer chemistry and applications. Saint-Quentin, France: Institut Géopolymère; 2008.
34. Gao P, Li S, Bu X, Dang S, Liu Z, Wang H, et al. Direct conversion of $CO_2$ into liquid fuels with high selectivity over a bifunctional catalyst. Nature Chem. 2017;9:1019–24. https://doi.org/10.1038/nchem.2794
35. Toniolo N, Rincón A, Avadhut YS, Hartmann M, Bernardo E, Boccaccini AR. Novel geopolymers incorporating red mud and waste glass cullet. Mater Lett. 2018;219:152–4. https://doi.org/10.1016/j.matlet.2018.02.061
36. Borra CR, Blanpain B, Pontikes Y, Binnemans K, Van Gerven T. Smelting of bauxite residue (red mud) in view of iron and selective rare earths recovery. J Sustain Met. 2016;2(1):28–37. https://doi.org/10.1007/s40831-015-0026-4
37. Chun T, Li D, Di Z, Long H, Tang L, Li F, et al. Recovery of iron from red mud by high-temperature reduction of carbon-bearing briquettes. J S Afr Inst Min Metall. 2017;117:361–4. https://doi.org/10.17159/2411-9717/2017/v117n4a7
38. Mombelli D, Barella S, Gruttadauria A, Mapelli C. Iron recovery from bauxite tailings red mud by thermal reduction with blast applied sciences iron recovery from bauxite tailings red mud by thermal reduction with blast furnace sludge. Appl Sci. 2019;9:4902. https://doi.org/10.3390/app9224902
39. Gu P, Beaudoin JJ, Quinn EG, Myers RE. Early strength development and hydration of ordinary portland cement/calcium aluminate cement pastes. Adv Cem Based Mat. 1997;6(2):53–8. https://doi.org/10.1016/S1065-7355(97)00008-4
40. MacDowell DE, Sorrentino F. Hydration mechanism of gehlenite glass cements. Adv Cem Res. 1990;3(12):143–52. https://doi.org/10.1680/adcr.1990.3.12.143
41. Passaglia E, Galli E. Vertumnite, a new natural silicate. Tsch Min Petr Mitt. 1977;24(1):57–66. https://doi.org/10.1007/BF01081745
42. Jackson MD, Landis EN, Brune PF, Vitti M, Chen H, Li Q, et al. Mechanical resilience and cementitious processes in Imperial Roman architectural mortar. Proc Nat Acad Sci. 2014;111(52):18484–9. https://doi.org/10.1073/pnas.1417456111
43. MacDowell JF. $CaO–Al_2O_3–SiO_2$ glass hydraulic cements. US Patent 4650443; 1986.
44. Dovál M, Palou M, Mojumdar SC. Hydrationbehavior of $C_2S$ and $C_2AS$ nanomaterials synthetized by sol–gel method. J Therm Anal Calorim. 2006;86(3):595–9. https://doi.org/10.1007/s10973-006-7713-0
45. Myers RJ, Bernal SA, San Nicolas R, Provis JL. Generalized structural description of calcium–sodium aluminosilicate hydrate gels: the cross-linked substituted tobermorite model. Langmuir. 2013;29(17):5294–306. https://doi.org/10.1021/la4000473

**How to cite this article:** Hujova M, Rabelo Monich P, Kankova H, Lucas H, Xakalashe B, Friedrich B, et al. New glass-based binders from engineered mixtures of inorganic waste. Int J Appl Glass Sci. 2021;00:1–11. https://doi.org/10.1111/ijag.16262